



Cite this: *Phys. Chem. Chem. Phys.*,
2020, 22, 17867

Spectroscopy and excited state dynamics of nearly infinite polyenes

Václav Šebelík,^a Miroslav Kloz,^b Mateusz Rebarz,^b Martin Přeček,^b
Eun-Hye Kang,^c Tae-Lim Choi,^c Ronald L. Christensen^{b,*d} and
Tomáš Polívka^{b,*a}

Steady-state and transient absorption spectra with <50 fs time resolution were obtained for two conjugated polymers, both with ≈ 200 conjugated double bonds (N), constrained in planar, stable, polyene frameworks. Solutions of the polymers exhibit the same $S_2 \rightarrow S_1 \rightarrow S^* \rightarrow S_0$ decay pathway observed for the $N = 11$ –19 polyene oligomers and for zeaxanthin homologues with $N = 11$ –23. Comparisons with the excited state dynamics of polydiacetylene and a much longer, more disordered polyene polymer (poly(DEDPM)) show that the S_2 , S_1 , and S^* lifetimes of the four polymers are almost identical. The S^* signals in the polymers are assigned to absorption from vibrationally excited ground states. In spite of significant heterogeneities and variations in conjugation lengths in these long polyenes, their $S_0 \rightarrow S_2$ absorptions are vibronically-resolved in room temperature solutions with electronic origins at ≈ 600 nm. The limiting wavelength for the $S_0 \rightarrow S_2$ transitions is consistent with the persistence of bond length alternation in the electronic ground states and a HOMO–LUMO band gap in polyenes with $N \approx 200$. The coincidence of the well-resolved $S_0 \rightarrow S_2$ electronic origins and the convergence of the excited state lifetimes in the four polymers point to a common, “nearly infinite” polyene limit.

Received 6th May 2020,
Accepted 28th July 2020

DOI: 10.1039/d0cp02465a

rsc.li/pccp

Introduction

Linear polyenes are organic molecules containing \sim one-dimensional, conjugated π -electron systems with alternating carbon–carbon bond orders in their electronic ground states. The unique electronic properties of polyenes and carotenoids, *e.g.*, the energies and dynamics of their excited electronic states, primarily depend on their length of conjugation. As a first approximation, the transition energies scale as $1/N$ where N is the number of conjugated C=C bonds, *e.g.*, $N = 11$ for β -carotene, lycopene, and zeaxanthin.^{1–5} Naturally occurring polyenes such as retinal ($N = 6$) serve as chromophores in vision and in phototrophic archaea,⁶ and longer carotenoids function as light-harvesting and/or photoprotective pigments in photosynthetic bacteria and plants.^{7–11} Carotenoids also quench chlorophyll triplet states, preventing damage due to the photosensitization of singlet oxygen.¹² Long or “infinite” polyenes have potential applications in optoelectronic devices as insulated, semiconductors/molecular wires, and there has

been considerable interest in the electronic properties of polyacetylene ($N = \infty$), polydiacetylene ($N = \infty$) and their substituted derivatives.^{13,14} Significant theoretical challenges remain in describing the correlated, delocalized π -electrons in linear polyenes, and the computational complexity scales nonlinearly with N . There also is extensive literature on other conjugated polymers and their oligomers, including PPV (poly(*p*-phenylene vinylene))^{13,15} and PPP (poly(*para*-phenylene)).¹⁶ But the chemistry and photophysics of these systems are quite different than those of the polyene oligomers, and we focus on long polyenes in this paper.

The extensive work on the spectroscopy of linear polyenes over the past five decades has been reviewed.^{5,17,18} Recent polyene history begins in 1972 with the discovery of the low-lying $2^1A_g^-$ (S_1) state.^{19,20} This electronic state lies below the $1^1B_u^+$ state corresponding to the HOMO \rightarrow LUMO transition ($1^1A_g^- \rightarrow 1^1B_u^+$, $S_0 \rightarrow S_2$) in simple versions of molecular orbital theory.²¹ Although the $1^1A_g^- \leftrightarrow 2^1A_g^-$ transitions are symmetry forbidden, shorter polyenes have relatively large $2^1A_g^- \rightarrow 1^1A_g^-$ ($S_1 \rightarrow S_0$) emission yields, and the $S_0 \rightarrow S_1$ absorptions have been readily detected for $N = 4$ –8 using fluorescence excitation techniques.^{17,22–25} These experiments are facilitated by incorporating the polyenes into low-temperature mixed crystals. This gives highly-resolved vibronic spectra as well as stronger emissions, *e.g.* the fluorescence yields approach unity for model tetraenes,²⁶ and significantly enhances both the

^a Institute of Physics, Faculty of Science, University of South Bohemia, České Budějovice, Czech Republic. E-mail: tpolivka@jcu.cz

^b ELI Beamlines, Institute of Physics, Czech Academy of Sciences, Za Radnicí 835, 252 41 Dolní Břežany, Czech Republic

^c Department of Chemistry, Seoul National University, Seoul 08826, Korea

^d Department of Chemistry, Bowdoin College, Brunswick, Maine 04011, USA. E-mail: rchrste@bowdoin.edu

selectivity and sensitivity of fluorescence excitation spectroscopy. Centrosymmetric, *all-trans* model polyenes also have been studied as cold, isolated (unsolvated) molecules in supersonic jets.^{27,28} The $1^1A_g^- \rightarrow 2^1A_g^-$ (and $2^1A_g^- \rightarrow 1^1A_g^-$) vibronic spectra are dominated by combinations of totally symmetric (a_g) C–C and C=C stretching modes, reflecting the rearrangement of the CC bond orders in different electronic states. Comparison of the high-resolution one-photon ($g \rightarrow g$ forbidden) and two-photon ($g \rightarrow g$ allowed) excitation spectra of molecules belonging to the C_{2h} point group, e.g., *all-trans* octatetraene in supersonic expansions, confirms that the one-photon transition is allowed by Herzberg–Teller vibronic coupling between $1^1B_u^+$ and $2^1A_g^-$ states *via* low frequency, in-plane b_u bending modes. For two-photon excitation, $1^1A_g^- \rightarrow 2^1A_g^-$ is symmetry-allowed with a relatively strong (0–0) transition.^{27,28} The electronic origin (0–0) is rigorously forbidden for one-photon absorption, and the one-photon spectra are offset from the two-photon spectra by the frequencies of at least four b_u promoting modes. There is no overlap between more than 150 vibronic bands observed in the one-photon spectrum and the two-photon spectrum of *all-trans* octatetraene.²⁷ Asymmetric substitution, e.g., in *all-trans* nonatetraene, results in considerable overlap of the one- and two-photon spectra with significant intensity in the one-photon electronic origin.²⁸ Analysis of the $S_0 \rightarrow S_1$ ($1^1A_g^- \rightarrow 2^1A_g^-$) transitions for these molecules provides a rigorous proof of the symmetry-forbidden nature of this electronic transition and the need to describe both the electronic and vibrational states by the irreducible representations of the C_{2h} point group.

Naturally occurring polyenes, e.g., carotenoids ($N \approx 5$ –13), are less amenable to rigorous spectroscopic or theoretical analysis than their simpler, more symmetric, model polyene counterparts. Their electronic spectra tend to be broader, in large part due to the distributions of conformations and nonplanarities imposed by methyl substituents along the polyene chains, especially by steric interactions between the polyene chains and methyl groups on terminal β -ionylidene rings.²⁹ Open-chain, diapocarotenoids such as lycopene ($N = 11$) have better resolved, red shifted $S_0 \rightarrow S_2$ absorptions compared to carotenoids with terminal rings such as β -carotene or zeaxanthin ($N = 11$). To account for the impact of the distortions and nonplanarities of the polyene chains, the concept of an effective conjugation length (N_{eff}) often has been employed.^{4,30–33} It also should be stressed that many carotenoids of photobiological interest have geometries for which the C_{2h} symmetry designations may not be appropriate in describing how electronic transitions are forbidden or allowed, or in describing excited state decays.^{34–37}

Absorption, emission, and excitation spectra of natural carotenoids and their analogs exhibit only the broad envelopes of the C–C and C=C vibronic combinations bands observed in the high-resolution spectra of model polyenes. This and diminishing fluorescence yields posed some initial challenges in the direct detection of the S_1 ($2^1A_g^-$) state in longer systems, and the S_1 state often has been described as “invisible” or “dark” in more-photobiologically relevant carotenoids. Nevertheless, a great deal has been learned from the optical spectra of these

molecules. Fluorescent yields are sufficient to locate the $S_1 \rightarrow S_0$ (0–0) bands in open-chain, *all-trans* diapocarotenoids with $N = 7$ –9.^{38–40} For *all-trans* diapocarotenoids with $N = 10$ –13, transient absorption measurements ($S_1 \rightarrow S_n$) yield S_1 lifetimes, and the energy gap law gives estimates of S_1 energies that are consistent with the S_1 energies and lifetimes of shorter members of the $N = 7$ –13 series.³⁹ The S_1 lifetimes of the diapocarotenoids range from ≈ 400 ps for $N = 7$ to ≈ 1 ps for $N = 13$. (*cf.* the 450 ns lifetime of the zero-point level of $2^1A_g^-$ in isolated *all-trans* octatetraene²⁸). This reflects the systematic increase in $S_1 \rightarrow S_0$ nonradiative decay rates and the decrease in $S_1 \rightarrow S_0$ fluorescence yields with increasing N . The fluorescence of longer polyenes and carotenoids is dominated by weak $S_2 \rightarrow S_0$ emissions with emission yields much less sensitive to conjugation length.³⁹ However, even for apo-carotenoids with terminal β -ionylidene rings, S_1 emissions can be detected for $N = 5$ –10, though accurate location of the $S_1 \rightarrow S_0$ electronic origins requires cooling solutions to 77 K to reduce conformational disorder and restore vibronic structure.⁴¹ In addition, the $2^1A_g^-$ states in carotenoids can be detected and zero-point energies determined from symmetry-allowed, $S_1 \rightarrow S_2$ transient absorptions in the near infrared.^{11,42} Both steady-state and transient absorption spectra demonstrate that the ordering of carotenoid electronic states ($E(2^1A_g^-) < E(1^1B_u^+):E(S_1) < E(S_2)$) for $N = 5$ –13 and their dynamics are consistent with extrapolations of the much more detailed data available for the short ($N = 4$ –8), symmetric, model polyenes.^{17,22–25}

Time-resolved studies of long, natural polyenes have suggested the existence of additional dark states in the excited state manifolds: longer carotenoids/polyenes have shorter lifetimes, and more complex relaxation pathways.³⁴ As first noted by Andersson and Gillbro⁴³ for long homologs of β -carotene ($N = 15$, $N = 19$), the $S_1 \rightarrow S_n$ band has a high-energy shoulder with a lifetime longer than the S_1 state. This feature originally was assigned to absorption from a vibrationally excited (“hot”) ground state. This band, commonly referred to as the S^* state, has been reported for a number of carotenoids, and its origin remains a controversial topic of carotenoid photophysics. Recent studies show that the S^* shoulder consists of signals originating both from vibrationally excited ground states and vibrationally relaxed S_1 states. For shorter ($N \leq 11$) carotenoids the S_1 contribution dominates, while for longer conjugated systems, the major contribution to the S^* signal appears to originate from hot ground states.^{44–47}

We previously studied high molecular-weight polymers of 1,6-heptadiene derivatives (poly(DEDPM)), polyenes with $N > 3000$, containing mixtures of five- and six-membered rings.^{48,49} These polymers exhibit significant conformational disorder, which can be reduced by cooling samples to 77 K, giving vibrationally resolved $S_0 \rightarrow S_2$ bands similar to those observed in carotenoids and model polyenes. The polymerization reactions lead to a broad distribution of conjugation lengths in the unpurified samples. However, the vibronically-resolved, red-shifted absorption at low temperature indicated that this distribution is dominated by species with very long conjugation lengths (N or N_{eff}) and similar $1/N \approx 1/N_{\text{eff}} (\approx 0)$. The work on

poly(DEDPM) was followed by a detailed study of the energies and dynamics of the low-lying electronic states of isomerically-pure oligomers ($N = 5-23$) with all five-membered rings.^{5,50,51} These molecules have constrained, planar polyene backbones, which reduce the impact of conformational disorder observed for substituted polyenes, carotenoids, poly(DEDPM), and polyacetylene. Steady-state and ultrafast transient absorption spectra reveal the N dependence of the energies of several $1^1A_g^- \rightarrow 1^1B_u^+$ transitions, which appear to converge to a common, infinite polyene limit of $\approx 16\,000\text{ cm}^{-1}$. Extrapolation of the S_1 state energies suggests a $\approx 10\,000\text{ cm}^{-1}$ energy in the long polyene limit.⁵ It should be noted that the $S_0 \rightarrow S_2$ transition energy (unlike the $S_0 \leftrightarrow S_1$ transition energy) is strongly dependent on solvent. This needs to be considered in comparing extrapolations of energies to infinite polyenes and carotenoids and also in evaluating theoretical treatments of excited state energies. The complex, multistep kinetics of the $S_2 \rightarrow S_1 \rightarrow S_0$ decay pathways of the oligomers were compared with the kinetic data from natural and synthetic carotenoids.^{43,52,53} The S_1 lifetimes are dominated by nonradiative decay, and the $S_1 \rightarrow S_0$ decay rates show remarkable parallels between the N dependences of the decay kinetics for carotenoids and the polyene oligomers.^{5,11} Distinctive transient absorption signals, identified with S^* states in several carotenoids, also were observed for the longer oligomers ($N > 11$).⁵

Chen *et al.*⁵⁴ recently reported the synthesis of *trans* polyacetylene using mechanical force (sonication) on polyadderenes. This elegant approach yields solutions of polyacetylene with $N > 100$ based on absorption and resonance Raman spectra, but the unresolved absorptions indicated a broad distribution of polyene lengths. Polyacetylenes synthesized in solution also tend to be unstable with the blue colors

associated with long conjugation lengths quickly fading. A promising alternative to synthesis in solution has been demonstrated by Hudson *et al.*^{14,55} The *in situ* synthesis of *trans*-polyacetylene in well-defined channels of urea inclusion complexes not only facilitates polymerization, but encases the conjugated double bonds in a secure, chemically inert environment. However, electronic spectra have not been reported for these samples.

This paper extends the work on the $N = 5-23$ oligomers to all five-membered ring polymers with $N > 200$ and with both small and large side chains (Fig. 1). Living polymerizations of 1,6-heptadiene derivatives using third-generation Grubbs catalysts have proven to be a powerful method for synthesizing very long polyenes with excellent selectivity toward five-membered rings in the polyene backbone.⁵⁶⁻⁵⁸ The first controlled living metathesis cyclopolymerizations were demonstrated by Schrock and co-workers in the early 1990s. Polymerizations of 1,6-heptadiyne monomers yielded polymers containing both 5- and 6-membered cycloalkenes in the backbone.⁵⁹ They later modified their catalysts to obtain 6-membered rings selectively.⁶⁰ Buchmeiser and co-workers expanded this chemistry and developed living polymerizations that gave only 5-membered rings.⁶¹ The polymers studied here reflect the significant synthetic advances over the past 25+ years and the ability to control the geometries of the double bonds and the distributions of conjugation lengths. The synthetic routes leading to **P1** and **P2** exploit the significantly higher solubilities of polymers with a variety of polar substituents to yield long conjugated polyenes. The cyclopolymerization method also allows the synthesis of polymers with bulky dendrons attached to each repeat unit.⁵⁶ Reduction of steric repulsions in **P1** and **P2** between the large side chains (R_1 and R_2) on the tetrahedral carbons results in three-dimensional structures

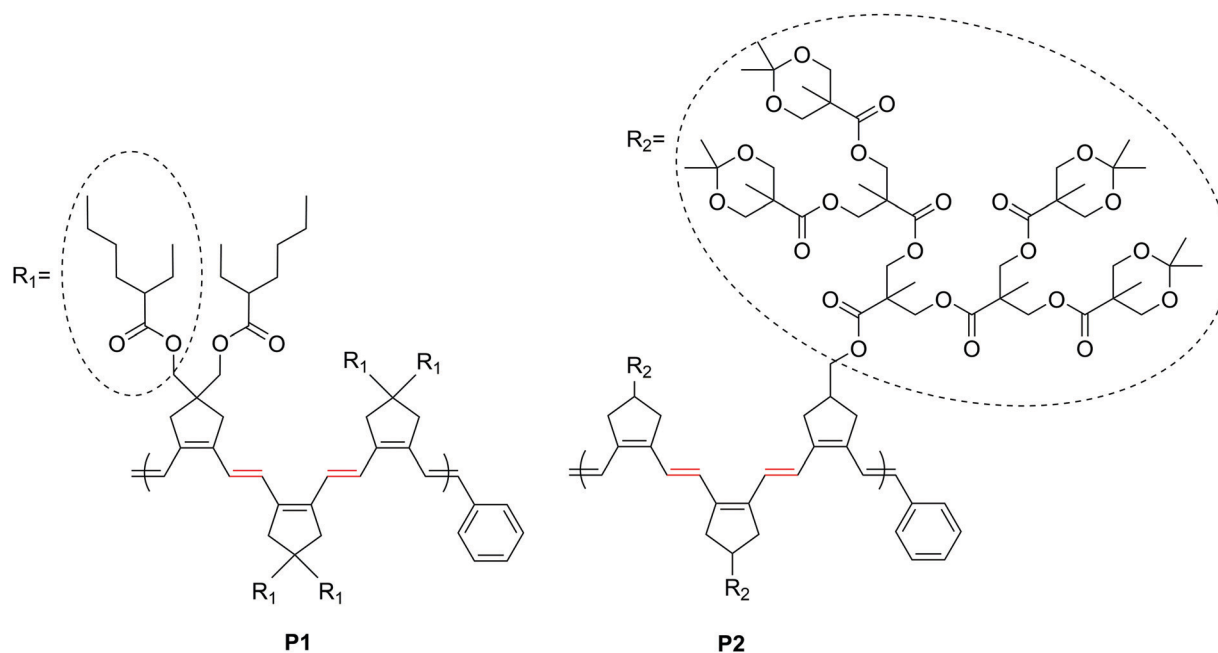


Fig. 1 Structures of **P1** and **P2**. The bonds in red denote the exocyclic double bonds, here in *trans*-configurations.

in which bulky substituents envelop the inner polyene core, leading to more linear, more extended polyene chains. The stabilities and high solubilities of these long polyenes allow their characterization and spectroscopic investigation in a range of solvents. Furthermore, the synthetic products can be aged/annealed to convert the small fraction of *cis* double bonds to *trans*, retaining the planar π -electron framework and giving very long linear polymers with rod-like morphologies. This notation (*trans* vs. *cis*) refers to the geometry of the central, exocyclic C=C bonds connecting the rings (red bonds in Fig. 1). The *all-trans* structures have been confirmed using NMR techniques and visualized by atomic force microscopy.⁶² In this paper we study the ground and excited state spectroscopy and dynamics of conjugated polymers **P1** and **P2** (Fig. 1) and compare with similar measurements on the $N = 5$ –23 oligomers and related natural and synthetic carotenoids. We also compare the spectroscopy and excited state dynamics of these polymers with recent studies of polyacetylene and polydiacetylene.

Materials and methods

Synthesis and characterization of polymers

The syntheses of the **P1** monomer and its polymerization have been presented previously.⁶² Similarly, the synthesis of the dendrimer-substituted monomer and its polymerization to **P2** have been described.⁵⁶ The polymerization reactions were followed using NMR and indicated $\approx 15\%$ of *cis* C=C bonds in the polyene chains. Central *cis* double bonds were converted to *trans* by exposure of room temperature solutions to UV/visible light and the isomerizations monitored using NMR techniques.⁶² 2-D proton NMR (COSY and NOESY) were used to identify structures with central *cis* structures versus structures with central *trans* structures. Well-resolved peaks associated with central *cis* structures disappear when converted to central *trans* structures. These changes correlate with the photochemical conversion of the $\sim 15\%$ of central *cis* bonds to give linear, “*all-trans*” structures.⁶² Both polymers are stable in room temperature solutions of acetonitrile and in BHT-stabilized tetrahydrofuran (THF). Samples stored as solids at $-80\text{ }^\circ\text{C}$ were stable for > 5 years with solution absorption spectra of reconstituted samples showing no evidence of decomposition from the time of their synthesis and characterization.

The molecular weights of **P1** and **P2** were estimated by size exclusion chromatography (SEC) and multi-angle laser light scattering (MALLS) as described previously.⁶² These measurements gave average molecular weights (M_n) of $\approx 52\,000$ for **P1** and $127\,000$ for **P2**. The weights of the monomer repeat units and the styrene end-capping group allows calculation of the degree of polymerization (DP) and the approximate number of double bonds in each polymer. The MALLS measurements also yield polydispersity indices (PDIs) for the two samples. The PDIs lead to estimates of the standard deviations of molecular weights and conjugation lengths.⁶³ For **P1**, $\text{PDI} = M_w/M_n = 1.49$, giving conjugation lengths ($N \pm 1\sigma$), $N = 260 \pm 180$ and for **P2**, $\text{PDI} = 1.11$;

$N = 230 \pm 80$. Note that $\sigma(N)/N = 0.70$ for **P1** and $\sigma(N)/N = 0.35$ for **P2**.

Spectroscopy

Transient absorption experiments were performed on a home built set-up installed at the ELI Beamlines laser user facility. It was based on 1 kHz Titanium Sapphire amplifier (Astrella, Coherent Co.) generating 34 fs pulses centered at 800 nm. The laser beam was split into a pump beam and a probe beam by a dielectric beam splitter. The pump beam excited commercial OPA (Topas Prime, Light Conversion Co.) generating 590 nm pulses with < 50 fs duration used for excitation of the sample. The probe beam pumped commercial dual OPA (Topas Twins, Light Conversion Co.) generating 1400 nm, < 50 fs pulses. These pulses were used to drive supercontinuum generation in a 2 mm thick CaF_2 plate, which was continuously translated in the beam to reduce the deposition of heat in the generation spot. A dichroic mirror with 350–1064 nm reflectivity (Semrock Co.) was used to separate the 350 to 1100 nm supercontinuum from the intense 1400 nm pump pulse. Pump and probe pulses were focused and overlapped on the sample with spot diameters of $\approx 40\text{ }\mu\text{m}$ for the probe and $\approx 120\text{ }\mu\text{m}$ for the pump. Sample thicknesses were 1 mm (\approx the Rayleigh length of the probe beam), held in the cuvette with 1 mm thick front and back quartz windows. The temporal delay between pump and probe pulses was adjusted by a remotely controlled optical delay line inserted in the pump beam before focusing into the sample. The temporal repeatability of the delay line was tested to be below 5 fs. Transient absorption signals were measured by a CCD camera (Entwicklungsbuero Stresing Co.) operated in full vertical binning, achieving shot-to-shot detection at 1 kHz. Two optical choppers were used: 500 Hz in the probe path and 250 Hz in pump path for correction for dark counts and scattering-luminescence. Chopper phases were directly fed into the detection system as a TTL signal to synchronize the data flow with the four-pulse sequence. The dwell time at each time delay was 2 s and several scans were collected to provide statistics adequate for the assessment of data quality.

All time-resolved data were fit globally using the software Glotaran (Vrije Universiteit Amsterdam). A sequential, irreversible scheme was assumed, in which the extracted time constants correspond to lifetimes of individual excited-states species. The resulting spectral profile of each kinetic component is called an evolution-associated difference spectrum (EADS). Although the EADS may not fully represent the complexity of all possible relaxation pathways, they carry important information about the excited-state dynamics.⁶⁴

Results and discussion

Ground state absorption

Absorption spectra of the two long polyenes are shown in Fig. 2. Only a single, vibronically-resolved electronic transition is observed, and this can be assigned to the dominant,

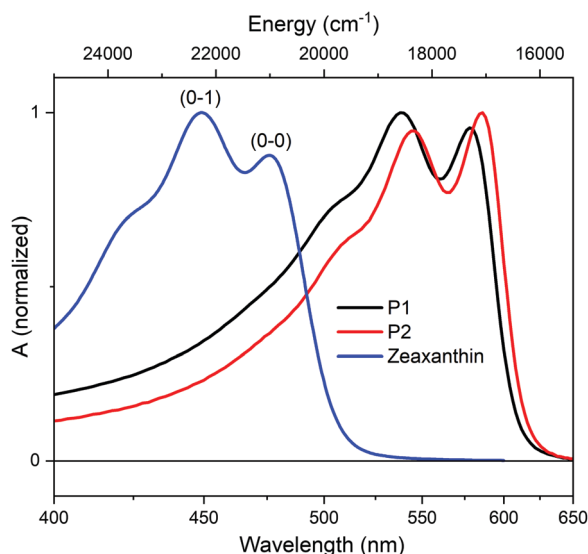


Fig. 2 Absorption spectra of **P1** (black) and **P2** (red) in acetonitrile compared with absorption spectrum of the carotenoid zeaxanthin in methanol (blue).

symmetry-allowed, $S_0 \rightarrow S_2$ transition ($1^1A_g^- \rightarrow 1^1B_u^+$ for C_{2h} polyenes) observed for shorter polyenes, including the $N = 5-23$ oligomers. Furthermore, the $\approx 17\,000\text{ cm}^{-1}$ transition energies for the (0-0) bands (580 and 587 nm) can be compared with extrapolation of the $N = 5-23$ oligomer (0-0) bands to the long polyene limit, $\approx 16\,000\text{ cm}^{-1}$.⁵ The presence of a single electronic transition in the polymer spectra also is consistent with the absorption spectra of the oligomers. At least six other $1^1A_g^- \rightarrow n^1B_u^+$ transitions are observed for the $N = 5-23$ oligomers,⁵¹ and the electronic origins of these relatively weak transitions appear to converge to the same $\approx 16\,000\text{ cm}^{-1}$ limit, collapsing the UV-Vis spectrum of the longest polyenes into a single, strong, vibronically-resolved, $S_0 \rightarrow S_2$ transition.⁵ There no doubt are additional, higher energy, 1^1B_u states in the oligomers, but these cannot be detected in the room temperature absorption spectra.^{5,51}

To emphasize the unusually well-resolved spectra of the room temperature solutions, we compare in Fig. 2 the absorption spectra of **P1** and **P2** with that of the carotenoid zeaxanthin ($N = 11$). Deconvolution of the spectra into sums of Gaussian components show that the (0-0) vibronic bands in **P1** and **P2** (FWHM = 945 and 865 cm^{-1}) are narrower than the (0-0) in highly purified zeaxanthin (FWHM = 1070 cm^{-1}). Carotenoid absorption spectra typically show a systematic loss of vibrational structure with increasing conjugation length due to the cumulative impact of ground state conformational disorder due to twisting and bending along the carbon-carbon chains.⁵² Out of plane distortions of the polyene chains lead to decreases in the effective length of conjugation ($N_{\text{eff}} < N$) and variations in N_{eff} result in a broader distribution of transition energies. For example, zeaxanthin ($N = 11$) and its $N = 15, 19, 23$, and 27 homologues exhibit a systematic loss of vibronic resolution with increasing N .^{52,65} The $S_0 \rightarrow S_2$ absorption spectra of $N = 5-23$ oligomers closely related to **P1** and **P2** show a similar

broadening with increasing N .⁵¹ This can be attributed to conformational disorder from out-of-plane twisting of the CCC torsional angles in room temperature solutions. Compared with carotenoids and other polyenes, the amplitudes of out-of-plane distortions in the oligomers should be constrained by the more rigid architecture of the all-five-membered ring systems. Disorder in the oligomers can be significantly reduced/eliminated by cooling solutions to 77 K, resulting in well-resolved $S_0 \rightarrow S_2$ spectra.⁵¹ This restores the planarities of the conjugated polyene chains and $N \cong N_{\text{eff}}$ for all species.

The differences in the absorption spectra of the two polymers (Fig. 2) merit comment. **P2** not only absorbs at longer wavelengths than **P1** but the relative intensities of the (0-0) and (0-1) bands are reversed in the two molecules. The vibronic intensities in **P2** are typical of “aged” samples for which the small fraction (15–20%) of *cis* double bonds from the living polymerizations were converted to *trans* configurations.⁶² The relatively strong (0-1) band in **P1** and the ≈ 7 nm blue shift suggests the presence of residual *cis* bonds and the possibility of a wider array of ground state geometries and N_{eff} in these samples. However, the **P1** absorption is within the range of spectra observed for related polymers that have been identified as aged, *all-trans* systems. For example, the absorption spectra of Poly(DHDPM)⁶² and a substituted fluorene derivative⁶⁶ have (0-0) bands in THF at 577 and 590 nm, respectively. **P1** and **P2** absorb within this range and the ratio of (0-0) and (0-1) intensities, rather than the position of the (0-0) band, probably is a better indication of the deviation of **P1** from an *all-trans*, planar geometry. Some of the small spread in the wavelengths of (0-0) bands in the *all-trans* polymers also might be traced to subtle differences in the electric fields felt by the polyene chains due to differences in polarities and polarizabilities of the large, enveloping substituents.

We also note our previous work on a related, high molecular weight ($N \approx 3300 \pm 800$) conjugated polymer (poly(DEDPM)) with a random mixture of five- and six-membered rings along the polyene chain.⁴⁸ This polymer does not share the approximate planarities of the conjugated carbon chains in **P1** and **P2**, and the room temperature, $S_0 \rightarrow S_2$ absorption of poly(DEDPM) in solution is broad and unresolved. However, cooling poly(DEDPM) to 77 K significantly reduces the conformational disorder, yielding a red-shifted, vibronically-resolved absorption with a 15 800 cm^{-1} electronic origin (FWHM $\approx 800\text{ cm}^{-1}$).⁴⁸ Similar red shifts upon cooling the longest oligomers ($\approx 900\text{ cm}^{-1}$ for $N = 23$)⁵¹ suggests a $< 600\text{ nm}$ (0-0) for poly(DEDPM) in room temperature 2-methyl-THF, comparable to the 580 and 587 nm origins for **P1** and **P2** in acetonitrile. These limiting wavelengths are consistent with the extrapolation of $1^1A_g^- \rightarrow 1^1B_u^+$ electronic origins in the $N = 5-23$ oligomers. This is the first instance where the $S_0 \rightarrow S_2$ transition energy of molecules approaching the infinite polyene limit can be systematically compared with trends observed in a homologous series of oligomers with a sufficient range of conjugation lengths to guide extrapolation. These comparisons are greatly facilitated by the vibronic resolution in the room temperature absorption spectra, even for polymers (**P1** and **P2**) with a wide range of conjugations lengths.

It is useful to compare the polymer absorption spectra and extrapolations to $N = \infty$ with solution spectra of polyacetylene (PA) and polydiacetylene (PDA) ($N \approx \infty$), though there is uncertainty about intra-chain disorder and the distribution of conjugation lengths in these samples.¹⁴ For example, the recent mechanochemical synthesis of polyacetylene in solution⁵⁴ produced polyenes (with large but unknown N s) with broad, unresolved, fleeting absorptions with maxima at ≈ 600 nm ($16\,700\text{ cm}^{-1}$) in THF. The absorption spectra extend to ≈ 850 nm ($11\,800\text{ cm}^{-1}$), but PA (and other long, *all-trans* polyenes) are notoriously insoluble in solution, and the red-shifted absorptions may be due to the formation of aggregates, microcrystals, or crossed linked polymers. The range of the $S_0 \rightarrow S_2$ polyacetylene absorption in solution is comparable with the spectrum of *all-trans* PA in neat, thin films,⁶⁷ which exhibits a broad absorption in the $\approx 12\,000$ – $16\,000\text{ cm}^{-1}$ range. We also note the absorption spectrum of the “blue” form of PDA with the conjugated chains aligned within a dilute matrix of the diacetylene monomer.⁶⁸ A strong zero-phonon line is observed at 635 nm, with higher energy vibronic peaks arising from symmetric stretches of the double and triple bonds. There thus is general agreement between the long polyene limit of the very soluble polymers studied here and of polyacetylenes and polydiacetylenes in solutions, thin films, and crystals. In addition, extrapolations of the (0–0) bands in a wide variety of natural and synthetic carotenoids suggest a 600–650 nm, infinite carotenoid limit.^{5,51,69,70} What these diverse polyenes have in common is a strong absorption at the red edge of the visible spectrum. The polymer samples described in this paper are distinguished by their well-characterized range of conjugation lengths (N), as well as their much higher solubilities and stabilities in a range of organic solvents. **P1** and **P2** thus offer significant advantages for probing the energies and dynamics of excited states in the long polyene limit.

The connections between the absorption data for **P1**, **P2**, poly(DEDPM), polydiacetylene, and various polyacetylenes and the (0–0) energies of the oligomers are further illustrated by Fig. 3. This compares the quadratic fit in $1/N$ to the (0–0) energies of the highly-purified $N = 5$ – 23 oligomers⁵ to a fit to a different, three-parameter empirical function to the (0–0)s of five zeaxanthins with $N = 11$ – 27 .⁶⁹ Although the two plots differ in the structures of the polyenes, the range (ΔE) of the fits, the fitting functions, and the solvents (2-methyl THF *vs.* dichloromethane), there is remarkable similarity in the curves. This includes their (probably fortuitous) convergence to almost identical asymptotic limits ($15\,900\text{ cm}^{-1}$ for the oligomers *vs.* $16\,050\text{ cm}^{-1}$ for the zeaxanthins). As noted above, these limits are in good agreement with the clustering of the (0–0) energies of **P1** and **P2** and other long polyenes at ~ 580 – 630 nm.

The resolution exhibited in Fig. 2 is a striking feature of the room temperature polymer absorptions. Polydispersity indices (PDIs) of the two polymers allow estimates of the standard deviations of polyene molecular weights and conjugation lengths,⁶³ giving $N = 260 \pm 180$ for **P1** and $N = 230 \pm 80$ for **P2**. The large range of high N s is compatible with well-resolved spectra, only if all molecules in the samples have essentially

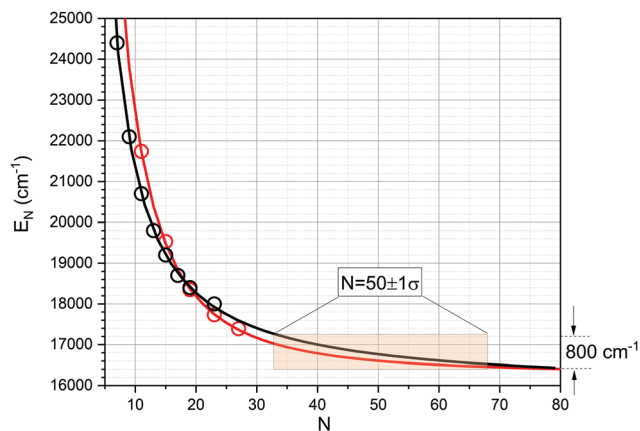


Fig. 3 Fits of N -dependence of the $S_0 \rightarrow S_2$ (0–0) energies parametrized for zeaxanthin series (red line)⁶⁹ and for oligomers (black line).⁵ The experimental values, taken from ref. 5 and 69, are denoted by open circles: red, zeaxanthin series in dichloromethane, black, oligomers in 2-MTHF. $1\sigma = 18 (=0.35N)$ as described in the text.

identical transition energies. This is consistent with the approximate $1/N$ dependence of the transition energies on conjugation length shown in Fig. 3. The quadratic fit to the energies gives $dE(N)/dN \approx -41\,000\text{ cm}^{-1}/N^2$ for large N .⁵ The difference between the transition energies of species with different N or N_{eff} thus becomes negligible for polyenes with sufficiently large N or N_{eff} . This also implies that the (0–0) transition energies of these polymers are not a useful diagnostic for detecting ground state conformational disorder. Conversely, the typically broad $S_0 \rightarrow S_2$ spectra observed for all published preparations of polyacetylene and other disordered, long polyenes indicates a much more heterogeneous collection of shorter polyenes, including conformationally disordered species. For example, the broad, blue-shifted absorptions of conjugated polymers with all-six-membered rings are dominated by polyene segments with $N_{\text{eff}} < 20$.⁷¹ Note that the above argument for the well-resolved absorptions in **P1** and **P2** does not hinge on the precise mathematical dependence of transition energies as a function of N ,^{69,70} only that the transition energies approach an asymptotic limit for large N .

Previous work on long, conformationally disordered polyenes⁷¹ raises the question of the minimal conjugation length consistent with the spectroscopic data for **P1** and **P2**. Although the molecular weights and PDIs indicate conjugation lengths of 260 ± 180 (**P1**) and 230 ± 80 (**P2**), the “spectroscopic units” or N_{eff} may be shorter due to conformational disorder or chemical breaks/defects in the conjugation. In Fig. 3 we use the quadratic fit to the transition energies to estimate that a collection of oligomers with $N_{\text{eff}} = 50 \pm 1\sigma$ (50 ± 18 based on the smaller PDI for **P2**: $\sigma(N)/N = 0.35$) would result in an $\sim 800\text{ cm}^{-1}$ range of (0–0) transition energies. This can be compared with the 945 and 865 cm^{-1} FWHM of the (0–0)s of **P1** and **P2**. These band widths are the result of both homogeneous and inhomogeneous broadening, including the impact of inhomogeneous solvent effects and conformational disorder. We thus expect that the contributions to the bandwidths due to

the heterogeneity in N or N_{eff} must be significantly less than 800 cm^{-1} . While our spectroscopic techniques and the uncertainties in the extrapolations do not allow the precise delineation of the N_{eff} or N at which we can refer to a “nearly infinite” polyene, the narrow (0–0) band widths for these heterogeneous polymers imply that the average N_{eff} must be greater than 50 for both **P1** and **P2**.

The analysis outlined above and illustrated in Fig. 3 relies on the assumption that $\sigma(N_{\text{eff}})/N_{\text{eff}} \approx \sigma(N)/N$. Interruptions in conjugation lengths due to synthetic defects, degradation of double bonds, or conformational disorder should be randomly positioned along the polyene chain. Given the architecture of these molecules, it is unlikely that low amplitude, out-of-plane torsions along the constrained polyene backbone would result in significant breaks in conjugation. Also, defects in the metal-catalyzed living polymerizations would terminate the polymerizations at a given N and not result in re-initiation of the polymerization or the production of short polyene segments. Regardless of the source of conjugation breaks, we assume that the fractional distribution of conjugation lengths derived from the PDIs ($\sigma(N)/N$ where N is the average N) would propagate/scale into comparable values for $\sigma(N_{\text{eff}})/N_{\text{eff}}$. The absorption spectra and excited state dynamics (see below) of **P1** and **P2** indicate that there are not significant, detectable populations of species with “small” N_{eff} in these samples, *e.g.*, we see no evidence of polyenes with $N_{\text{eff}} < 30$. **P1** and **P2** thus are in a regime where the number of breaks in conjugation, starting with $N \approx 200$, must be relatively small, and the approximation ($\sigma(N_{\text{eff}})/N_{\text{eff}} \approx \sigma(N)/N$) will be most valid for large N_{eff} . Given the uncertainties in estimating $\sigma(N_{\text{eff}})/N_{\text{eff}}$, we have taken a conservative approach in Fig. 3 by using the smaller of the relative uncertainties in the conjugation length ($\sigma(N_{\text{eff}})/N_{\text{eff}} \approx 0.35$ for **P2**) and a low threshold ($N = 50$) for the minimum average N_{eff} . Using the quadratic fit and $\sigma(N_{\text{eff}})/N_{\text{eff}} \approx \sigma(N)/N = 0.70$ for **P1** gives $N \approx 50 \pm 35$, which leads to a $\sim 2800 \text{ cm}^{-1}$ span in (0–0) energies. This is significantly larger than the $< 1000 \text{ cm}^{-1}$ bandwidths observed for **P1** and **P2**. Even for $N_{\text{eff}} \approx 100 \pm 70$, the (0–0) band of **P1** would have an estimated width of $\sim 1250 \text{ cm}^{-1}$. We also should emphasize that the data presented in this paper do not preclude the possibility that $N_{\text{eff}} = N$ and $\sigma(N_{\text{eff}}) = \sigma(N)$, *i.e.*, that the conjugation lengths for **P1** and **P2** are 260 ± 180 and 230 ± 80 , as derived from the molecular weights.

Excited state absorption and dynamics

Transient absorption spectra following excitation of the polymer $S_0 \rightarrow S_2$ (0–0) bands are presented in Fig. 4. Excitation into the electronic origins ($\approx 590 \text{ nm}$) eliminates the dynamics associated with decay of the S_2 vibrational states. The two long polyenes exhibit very similar kinetics with ground state bleaching below 600 nm and broad, excited state absorption extending beyond 1100 nm . The excited state dynamics can be separated into three spectral regions, each exhibiting different kinetic behavior. The spectral region above 900 nm shows the fastest decay and it is related to the excited state absorption ($S_2 \rightarrow S_m$) from the zero-point level of the S_2 state with

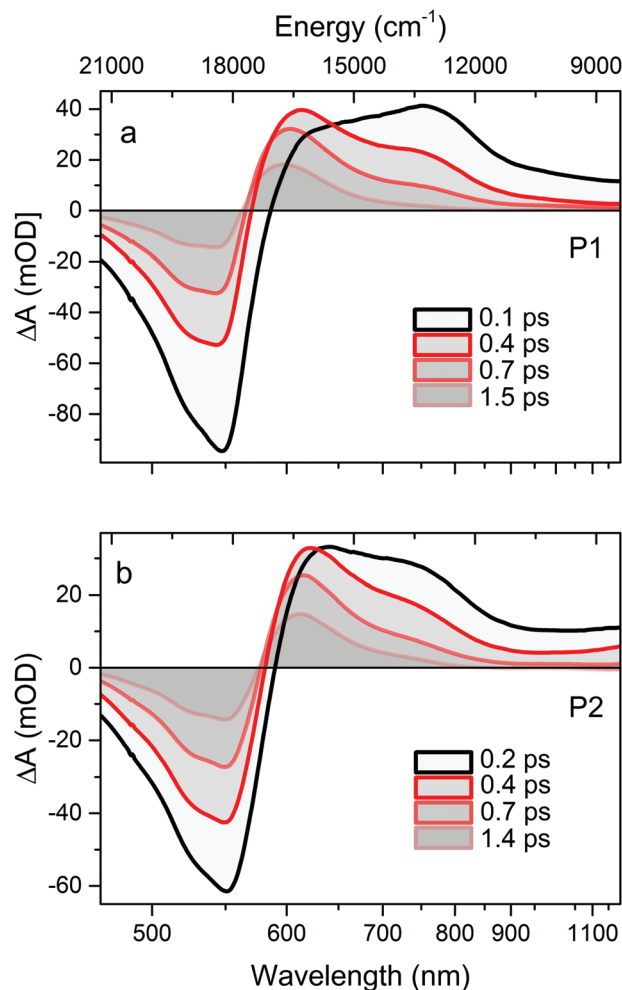


Fig. 4 Transient absorption spectra of **P1** (a) and **P2** (b).

the $\approx 50 \text{ fs}$ decay reflecting the S_2 lifetime. A slower decay ($\approx 300 \text{ fs}$) is associated with the band peaking at $\approx 750 \text{ nm}$ for **P1** and $\approx 760 \text{ nm}$ for **P2**. Based on comparisons with the constrained oligomers⁵ and long zeaxanthins,⁵² this feature is assigned to the characteristic $S_1 \rightarrow S_n$ transition ($1^1A_g^- \rightarrow n^1B_u^+$ for C_{2h} polyenes). The excited state absorption bands at 620 nm (**P1**) and 630 nm (**P2**) decay more slowly ($\approx 2 \text{ ps}$) than the 760 nm bands. Comparison with similar signals reported for a number of carotenoids^{44–47} and the longer ($N \geq 13$) oligomers,⁵ leads to the assignment of S^* states for these transient signals.

Differences in the dynamics of various spectral regions are further demonstrated by the kinetics of the transient absorption signals (Fig. 5). Distinct decays are evident within the $S_2 \rightarrow S_m$ band (1100 nm), $S_1 \rightarrow S_n$ band ($\approx 750 \text{ nm}$) and S^* band ($\approx 620 \text{ nm}$). The kinetics measured in the bleaching band at $\approx 550 \text{ nm}$ contains components associated with decays of the S_1 and S^* signals, suggesting that both states contributes to ground state recovery. To determine the time constants of the individual processes, we applied a global fitting analysis⁶⁴ to the full spectro-temporal data sets. Using a simple sequential model ($S_2 \rightarrow S_1 \rightarrow S^*$), we obtained the Evolution Associated

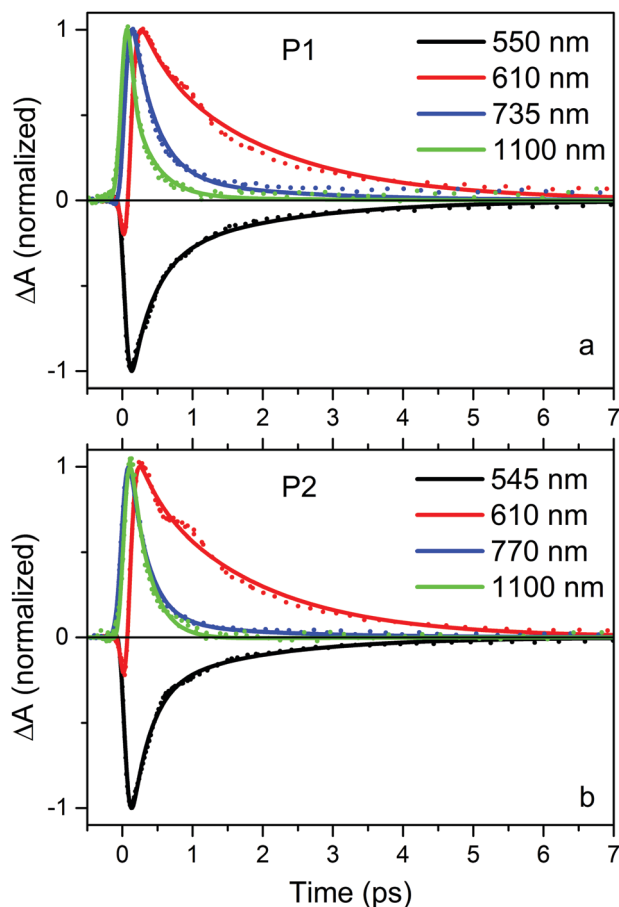


Fig. 5 Normalized kinetics (dots) with fits obtained from global fitting analysis (solid lines) of **P1** (a), and **P2** (b) at different wavelengths.

Difference Spectra (EADS) shown in Fig. 6 and extracted the lifetimes of the three states. The first EADS (black) is the spectrum corresponding to the initially excited, S_2 state. This contains a negative band due to ground state bleaching and stimulated emission from the S_2 state, as well as the positive band above 800 nm due to $S_2 \rightarrow S_m$ absorption. There is no significant difference between the S_2 lifetimes of **P1** and **P2**: both are ≈ 50 fs.

The second EADS (red) represents the spectrum associated with the decay of the S_1 state. The extracted lifetimes are 265 fs for **P1** and 300 fs for **P2**. Short S_1 lifetimes are expected for polyenes with a very long conjugation lengths as evidenced by comparisons with constrained polyenes with $N = 19$ and the zeaxanthin homologue with $N = 23$ with S_1 lifetimes of 500 fs⁵ and 200 fs.⁵² Antognazza *et al.*⁴⁹ reported a 175 fs S_1 lifetime for the closely related, but more disordered poly(DEDPM) with $N > 3000$.

The longest-lived EADS (blue) is due to the S^* signal with its characteristic derivative-like shape exhibiting positive signal at wavelengths adjacent to the ground state bleaching. The lifetimes of the S^* signals, 1.6 and 1.8 ps for **P1** and **P2** are slightly shorter than the lifetimes reported for the $N = 19$ constrained polyene (2.7 ps)⁵ and the $N = 23$ zeaxanthin (2.3 ps).⁵² But, it should be noted that these reference molecules exhibit two

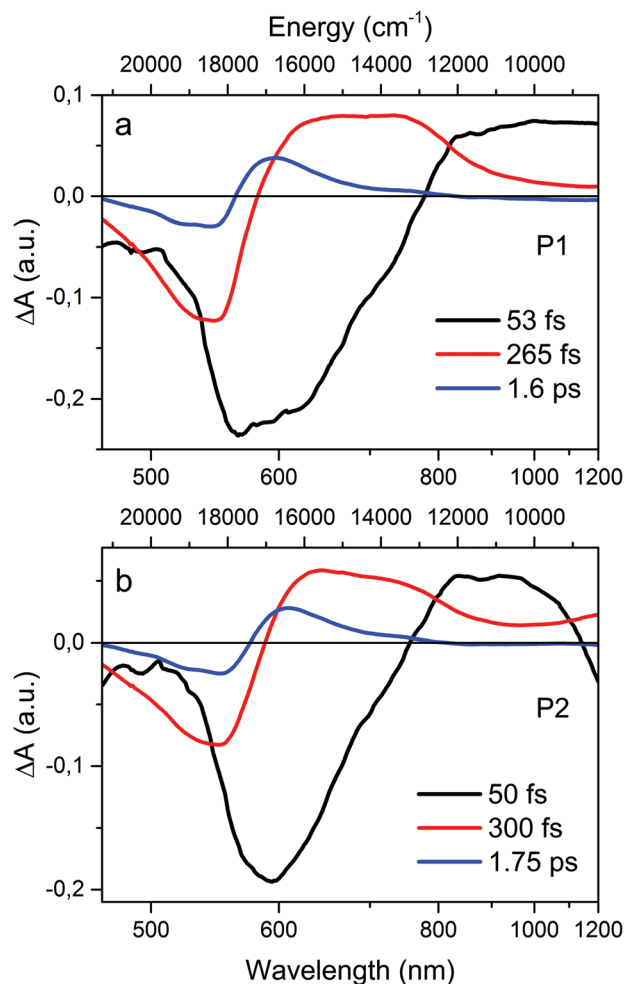


Fig. 6 EADS and lifetimes of S_2 , S_1 , and S^* obtained from global analysis of the data for **P1** (a), and **P2** (b).

spectrally similar S^* EADS components with different lifetimes,^{5,52} while for the **P1** and **P2**, only one S^* lifetime is required to obtain good fits. A single S^* lifetime (1.2 ps) also was reported for poly(DEDPM). This originally was assigned to the S_1 state,⁴⁹ but subsequent studies of polyenes and carotenoids with varying conjugation lengths showed that the long-lived decay was due to S^* .^{5,52} Comparisons of the S_2 , S_1 , and S^* lifetimes of **P1** and **P2** with relevant polyene oligomers and zeaxanthins are summarized in Table 1.

Fig. 7 compares transient absorption spectra of **P2** and zeaxanthin ($N = 11$), whose transient absorption spectra are shifted to match the maximum of the bleaching signal of **P2**. Note the significantly larger gap between the bleaching maxima and the $S_1 \rightarrow S_n$ maxima for **P1** and **P2**. This behaviour also was observed for the oligomers⁵ and synthetic long zeaxanthins.⁵² The spectral profiles of the $S_1 \rightarrow S_n$ and S^* bands for **P1** and **P2** are much broader than those of the corresponding bands in zeaxanthin (Fig. 6/ Fig. 7), in striking contrast to the ground state absorptions (Fig. 2). The narrow $S_0 \rightarrow S_2$ absorption profiles of **P1** and **P2** were attributed to the $\approx 1/N$ dependence of the $S_0 \rightarrow S_2$ transition energy. The wide distribution of

Table 1 S_2 , S_1 , and S^* lifetimes and S_2 energies of conjugated polymers, polyene oligomers, and carotenoids

Molecule	(0-0) S_2 energies (cm^{-1})	τ (S_2) (fs)	τ (S_1) (ps)	τ (S^*) (ps)	Ref.
P1	17 241	53	0.27	1.6	This work
P2	17 036	50	0.30	1.8	This work
Poly(DEDPM) ^a	15 800 ^b	51	0.18	1.2	Antognazza <i>et al.</i> ⁴⁹
Polydiacetylene ^c	15 748	320	0.38	2.3	Pandya <i>et al.</i> ⁶⁸
$N = 19$ oligomer ^d	18 400	100	0.49	2.7/0.67 ^e	Christensen <i>et al.</i> ⁵
$N = 15$ oligomer	19 200	90	1.1	6.9	Christensen <i>et al.</i> ⁵
$N = 13$ oligomer	19 800	130	2.3	5.0	Christensen <i>et al.</i> ⁵
$N = 11$ oligomer	20 700	120	6.1		Christensen <i>et al.</i> ⁵
Z23 ($N = 23$) ^f	16 560	<100	0.19	2.3/0.24 ^e	Staleva <i>et al.</i> ⁵²
Z19 ($N = 19$) ^f	17 095	<100	0.35	1.6	Staleva <i>et al.</i> ⁵²
Z15 ($N = 15$) ^f	18 280	<100	0.9	2.9	Staleva <i>et al.</i> ⁵²
Zeaxanthin ($N = 11$)	20 450	135	9.0	9.0	Staleva <i>et al.</i> ⁵²
Rhodoxanthin ($N = 14$) ^g	19 881	<100	1.1	5.6	Chábera <i>et al.</i> ⁷⁴
Spirilloxanthin ($N = 13$) ^h	19 048	100	1.4	6	Gradinaru <i>et al.</i> ⁷⁵

^a Note the different assignment of the time constants in Antognazza *et al.* 2010. The 1.2 ps decay originally was assigned to the S_1 lifetime, while the 0.18 ps decay was attributed to the relaxation of a vibrationally excited S_1 state. ^b From ref. 48, measured at 77 K. The estimated value at RT is $\sim 16\,800\text{ cm}^{-1}$ based on temperature-induced shifts reported for oligomers.⁵¹ ^c Polydiacetylene (PDA) embedded in crystal of the diacetylene monomer. ^d All oligomers measured in 2-MTHF. ^e Decay is multiexponential, and two components are necessary to fit the data in the S^* spectral region. ^f Synthetic homologues of zeaxanthin measured in THF. ^g In benzene. ^h In hexane.

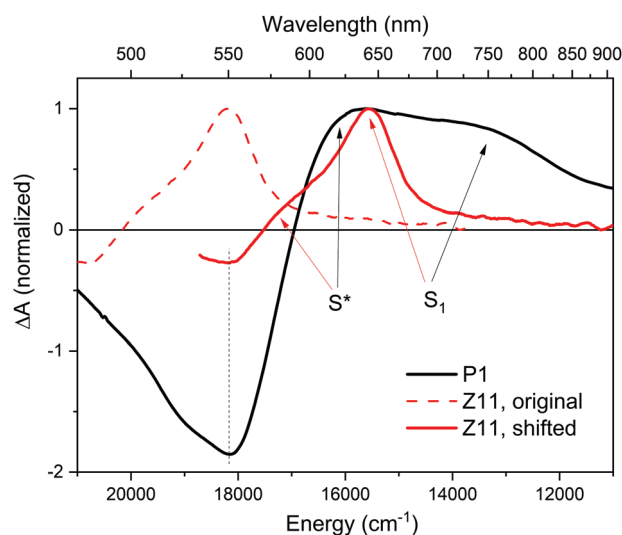


Fig. 7 Comparison of normalized transient absorption spectra of **P2** (black), and zeaxanthin ($N = 11$, red). The zeaxanthin spectrum is shown as original data (dashed), and shifted to match the bleaching of **P2** (solid). The spectral bands corresponding to the S^* and S_1 states are marked by arrows.

conjugation lengths (N and N_{eff}) and conformational disorder in these samples impact the transition energy only marginally for large N , resulting in almost identical $S_0 \rightarrow S_2$ absorptions for all species and conformations.

The broadness of the $S_1 \rightarrow S_n$ and S^* bands might be attributed to a different dependence of S_n and S^* energies on N_{eff} in the long polyene limit, yielding a larger range of transition energies in these heterogeneous samples. Other effects, such as large geometry changes involving more significant reordering of carbon-carbon bond lengths in S_1 and S_n , giving wider, unresolved, Franck-Condon envelopes also may

play a role. The relatively short S_1 and S^* lifetimes may prevent the completion of vibrational relaxation within these states for polyenes with large N . We note recent studies of the transient absorption spectra of PDA, which shows a $S_1 \rightarrow S_n$ absorption similar to that in **P1**, **P2**, and poly(DEDPM). The signals in PDA have been attributed to the existence of spatially separated triplet pairs ($^1(\text{TT})$) within the doubly-excited configurations in the S_1 (2^1A_g^-) state.⁶⁸ Coulombic interactions may lead to a broad range of $^1(\text{TT})^*$ excited states ($^1\text{B}_u$ in the C_{2h} point group), especially in longer polyenes. These states have different geometries and a distribution of triplet separation distances, leading to broadening in the transient absorptions.

The intensities of the S^* signals in **P1** and **P2** (and in poly(DEDPM) and PDA) are much stronger than in zeaxanthin (see Fig. 7), relative to those assigned to $S_1 \rightarrow S_n$ absorptions. Hints of these trends are suggested by the relative intensities of S^* and $S_1 \rightarrow S_n$ signals in the transient absorption of longer members of the $N = 5$ –23 oligomer series⁵ as well as in longer synthetic zeaxanthins.⁵² However, the S^*/S_1 ratio is sensitive to the time delay in the observation of the transient spectra. Given the limited information available in these broad spectra, we are not able to assess the competing scenarios for the significantly broadened, S^* signals in **P1** and **P2**.

The S_1 (2^1A_g^-) $\rightarrow S_n$ transitions for **P1** and **P2** terminate in states $13\,000$ – $14\,000\text{ cm}^{-1}$ above S_1 (Fig. 6). Extrapolation of the S_1 energies observed for the $N = 5$ –23 oligomers suggested vibrationally relaxed S_1 (2^1A_g^-) states of **P1** and **P2** at $\approx 10\,000\text{ cm}^{-1}$. This places the S_n states of **P1** and **P2** at $\approx 23\,000$ – $24\,000\text{ cm}^{-1}$, considerably higher in energy than the extrapolations of the $^1\text{B}_u^+$ states detected in the oligomers, which appear to converge at $\approx 16\,000\text{ cm}^{-1}$ in the infinite polyene limit.^{5,51} The transient absorption signals of **P1** and **P2** (and of poly(DEDPM)) point to higher energy manifolds of $^1\text{B}_u^+$ states in the oligomers, which cannot be accessed *via*

one-photon excitation from the electronic ground states ($1^1A_g^-$), either due to vanishingly small oscillator strengths or to transition energies outside the range of our oligomer absorption measurements. Furthermore, the significantly different electronic structures of $1^1A_g^-$ and $2^1A_g^-$ argues that the $1^1B_u^+$ states accessed from S_1 most likely do not overlap with the set of $1^1B_u^+$ states accessed by one-photon excitation of S_0 . The 1^1B_u states populated *via* the S_1 - S_n transition will likely have significant contribution from the $1^1(TT)$ pairs (as the $2^1A_g^-$ state does), preventing detection of these high energy B_u^+ states in the ground state absorption spectrum.⁶⁸

Similarly, the S_2 ($1^1B_u^+$) \rightarrow $1^1A_g^-$ transition at $\approx 10\,000\text{ cm}^{-1}$ (Fig. 6) implies high energy $1^1A_g^-$ states for **P1** and **P2** at $\approx 26\,000$ – $27\,000\text{ cm}^{-1}$, well beyond the range of the two $1^1A_g^-$ states revealed (and extrapolated to $\approx 10\,000\text{ cm}^{-1}$ and $\approx 19\,000\text{ cm}^{-1}$ for the infinite polyene⁵) in the visible and near infrared transient absorption spectra of the oligomers. Our previous experiments and analysis of the $N = 5$ – 23 oligomer spectra⁵ thus oversimplify a more complex manifold of symmetry-allowed, but “dark”, electronic states, as well as symmetry-forbidden states. This points to the complexity of interpreting the one-photon absorption spectra originating from the S_0 , S_1 , and S_2 for both short and long polyenes. Nevertheless, the rich data set now available for the oligomers (*e.g.* ≈ 7 allowed electronic transitions originating from S_0) and for **P1** and **P2** reveal simplifying patterns that deserve further theoretical attention.

The lifetimes of the S_2 , S_1 , and S^* states of **P1**, **P2**, and poly(DEDPM) are compared with those of other long-conjugated polyenes, polydiacetylene, and both synthetic and natural carotenoids in Table 1. The sequential model ($S_2 \rightarrow S_1 \rightarrow S^*$) provides a good description of the dynamics for all of these polyenes and supports the hypothesis that for longer polyenes/carotenoids the S^* signal is dominated by absorption from a vibrationally excited ground state populated *via* $S_1 \rightarrow S_0$ internal conversion. While for carotenoids with $N_{\text{eff}} \leq 11$, modelling the S^* signal requires significant contribution from the S_1 state,^{44,46} in longer systems the S^* signal can be explained as nearly exclusively due to a hot ground state.⁴⁵ The S_2 and S^* lifetimes are not strongly dependent on N , but the S_1 lifetimes decrease with increasing N , as previously noted for the $N = 5$ – 23 oligomers, open-chain carotenoids, and β - β -carotenoids such as the zeaxanthins.^{5,11,39,52} The $S_1 \rightarrow S_0$ nonradiative decay rates of the $N = 7$ – 19 oligomers were analyzed using the energy gap law (the S_1 - S_0 energy gap decreases with $\approx 1/N$), suggesting a ~ 40 fs S_1 lifetime estimate for the infinite polyene.⁵ The 175–400 fs S_1 lifetimes of the **P1**, **P2** and PDA are considerably longer. The extrapolation of the S_1 lifetimes to the infinite limit thus is more complicated than the extrapolation of the S_2 energy, *i.e.*, an asymptotic limit appears to be approached at smaller N . One explanation is that S_1 - S_0 relaxation likely occurs through a conical intersection,⁷² and vibrational coupling between the S_1 and S_0 states plays an important role in facilitating S_1 - S_0 internal conversion.⁷³ Thus, the time scales in which long polyenes convert electronic energy into vibrational energy may represent a physical limit for the S_1 lifetime. This limit precludes the application of simple extrapolations for estimating the S_1 lifetimes

for very large N .⁵ Nevertheless, the S_1 lifetimes of the oligomer and carotenoid series provides useful guidelines for understanding radiationless decay in **P1**, **P2**, and other conjugated polymers with very large N . The kinetic data summarized in Table 1 also emphasizes the striking similarities between radiationless decay processes from the S_2 , S_1 , and S^* states in the longer oligomers and corresponding longer carotenoids. The excited state lifetimes primarily are determined by N (or N_{eff}), rather than by the subtle structural details or the symmetries of these linearly conjugated molecules.

The peripheral substituents in **P1** and **P2** have little impact on their excited state decays (Table 1). Dendronized “*all-trans*” **P2** should have the most ordered and extended π -electron chains. **P1**, on the other hand, has a significant fraction of *cis* double bonds, which presumably results in sterically-hindered segments with less-planar polyene chains and a less linear secondary structure. These macroscopic differences can be related to the transition from coil to rod morphologies when the $\approx 16\%$ of *cis* double bonds of a related conjugated polymer (poly(DHDPM)) were converted to *trans*.⁶² This transformation had a significant impact on the absorption, red shifting the spectrum by 13 nm and increasing the vibronic resolution. These changes have been interpreted as relieving twists and nonplanarities in the polyene backbone, resulting in a more-linear, more-conjugated structure for the *all-trans* polymers. Poly(DEDPM) has a much higher N (≈ 3300) than **P1** or **P2** and a random sequence of 5- and 6-membered rings along the polyene chain. The larger disorder is reflected in its broad, unresolved absorption (and its high solubility) in room temperature solutions. In spite of significant structural differences, there is remarkable agreement in the dynamics extracted from the sequential model for **P1**, **P2**, and poly(DEDPM), and neither increasing N from ≈ 200 to ≈ 3000 nor introducing geometric or conformational disorder has significant impact on the excited state dynamics in the long polyene limit. Furthermore, there is good agreement between the dynamics of these polymer solutions and the sequential decay of the excited states of PDA in a highly-ordered, solid matrix.⁶⁸

Conclusions

Transient absorption spectroscopy with < 50 fs time resolution has provided a wealth of information about the ground and excited-state properties of polyenes with conjugation lengths approaching the long polyene limit. The constrained, conjugated polymers (**P1** and **P2**) used in this study offer several distinct advantages over previous samples of long polyenes purporting to approximate polyacetylene or polydiacetylene. These polymers are soluble in a range of organic solvents and have excellent thermal and photochemical stability in room temperature solutions. Their solutions thus are well-suited for a variety of analytical and spectroscopic studies, including ultrafast transient absorption studies requiring long data collection times. Solution NMR studies have confirmed the *all-trans* geometries of properly annealed/aged samples such as **P2**.⁶²

The large dendrimer substituents in **P2** encase the constrained, planar polyene core in a protective sheath, promoting elongated, linear, and stable structures. The bulky substituents in **P1** and **P2** effectively block intra- and intermolecular interactions between polyene chains, including cross-linking.

The stabilities and solubilities of these polymers allow size-exclusion chromatography (SEC) and light scattering measurements (MALLS) to estimate the distributions of molecular weights and conjugation lengths: $N \approx 260 \pm 200$ for **P1** and $N \approx 230 \pm 80$ for **P2**. For shorter polyene samples, a comparable range (35–75%) of conjugations lengths, plus the heterogeneities introduced by conformational disorder (even in these highly constrained molecules), would result in a broad superpositions of transition energies and excited state decays, making spectroscopic and kinetic studies untenable, or at least uninterpretable. However, the room temperature absorption spectra ($S_0 \rightarrow S_2$) are remarkably well-resolved, demonstrating that the broad range of conjugated species in these very heterogeneous samples have almost identical transition energies. This only can be true, if the conjugation lengths are sufficiently large for the spectra of all polyene components to converge to an asymptotic limit for large N , as expected for linear conjugated molecules with alternating carbon–carbon bond lengths. Previous studies^{5,51} of the $N = 5$ –23 oligomers of these polymers suggest an approximate $1/N$ dependence of observed transition energies on polyene length, and $1/N \cong 1/N_{\text{eff}} \cong 0$ for all species in the polymer solutions. The experiments described here thus explore the ground and excited-state properties of polyenes in the “almost infinite” limit.

The excited state dynamics of the conjugated polymers are very similar to the dynamics of their longer oligomers⁵ and of synthetic carotenoids with $N \geq 15$ ⁵² (Table 1). These comparisons provide further evidence that the photophysics of the S_2 , S_1 and S^* states, especially in the long polyene limit, primarily is determined by the number of conjugated C=C bonds, rather than more subtle structural details, including symmetry. The trends in the ground state and transient absorption spectra are quite similar for the oligomers ($N = 5$ –23) and the zeaxanthin series ($N = 11$ –23). The S_1 lifetimes systematically decrease with increasing N , approaching 200–400 fs in the long polyene limit. The 1–2 ps S^* lifetimes of **P1** and **P2** are slightly shorter than the ≈ 2 –9 ps lifetimes of the longer oligomers, zeaxanthin and its homologues, rhodoxanthin ($N = 14$), and spirilloxanthin ($N = 13$) (Table 1). Assignment of the S^* state to a hot ground state implies slightly faster vibrational cooling of the ground state in “nearly infinite” systems. Furthermore, the onset of the S^* signals for $N \geq 11$ and the dominant role of excited vibrational states of S_0 in accounting for these signals are consistent with the spectra and dynamics of the polymers.

It is instructive to compare the excited state kinetics of **P1** and **P2** with a related, extremely long ($N > 3000$) polyene poly(DEDPM).⁴⁹ All three polymers have very long conjugation lengths ($1/N \approx 0$), but there are significant structural differences. The interior double bonds in dendronized **P2** essentially are all in *all-trans* configurations giving highly ordered and extended/linear π -electron chains. **P1** contains a significant fraction of *cis* double

bonds, which presumably results in segments with less regular, less linear, secondary structures. Poly(DEDPM) has a much higher N than **P1** and **P2** and a random collection of 5- and 6-membered rings along the unconstrained polyene chains, leading to non-planarities and substantial disruption in the conjugation, especially in room temperature solutions. Yet, in spite of significant structural differences and the different levels of disorder and heterogeneities, the three polymers share very similar absorption spectra and excited state decays (Table 1). Another key conclusion of this paper is that the absorption spectra and dynamics of the S_2 , S_1 , and S^* states of these polymers in solution are very similar to what is observed for polydiacetylene (PDA) in an ordered matrix of its diacetylene monomer.⁶⁸

The four polymers (**P1**, **P2**, poly(DEDPM), and PDA) share similar electronic properties. Their S_2 , S_1 , and S^* lifetimes are almost identical (except for the S_2 lifetime of PDA) and appear to converge to a long polyene limit (Table 1). They exhibit the same $S_2 \rightarrow S_1 \rightarrow S^*$ kinetic scheme observed for the oligomers of **P1** and **P2** and for carotenoids with $N_{\text{eff}} > 12$,^{5,52} their $S_0 \rightarrow S_2$ absorptions are vibronically resolved with electronic origins at ≈ 600 nm. The limiting wavelength for the $S_0 \rightarrow S_2$ absorptions is consistent with bond length alternation in the electronic ground states and the persistence of a “band gap” in what appears to be the infinite polyene limit. Previous experimental results for “infinite” polyenes, *e.g.*, polyacetylene ($N \cong \infty$), more likely should be assigned to mixtures of polyenes with finite and uncertain polyene chain lengths.¹⁴ Similar issues arise for poly(DEDPM) and PDA. There are no estimates of conjugation lengths for PDA, and it is very unlikely that there are any segments with > 3000 conjugated double bonds in solutions of poly(DEDPM). Synthetic defects, chemical and photochemical degradation, cross-linking, and significant conformational disorder in these very long, very nonplanar systems almost certainly result in intramolecular distributions of considerably shorter segments. Nevertheless, the absorption spectrum of poly(DEDPM) is well-resolved at 77 K,⁴⁸ and the (0–0) band matches well with those of **P1**, **P2**, and PDA.⁶⁸ The coincidence of the well-resolved $S_0 \rightarrow S_2$ absorptions and the convergence of excited state lifetimes points to a common, long-polyene limit.

The synthesis of **P1** and **P2** represents a significant advance in living polymerization techniques. These polymers have all five-membered rings with a relatively rigid, locked, planar arrangement of conjugated double bonds. In spite of significant variations in their conjugation lengths, the constrained, planar structures gives vibronically-resolved absorptions, even in room temperature solutions. There are indications of minor conformational disorder, presumably due to low amplitude torsions along the polyene chains: the 77 K absorptions of the oligomers are even better resolved than the RT absorptions.^{5,51} The current studies thus are based on much improved synthetic strategies and well-characterized samples. Our analysis of the relatively narrow band widths of **P1** and **P2** indicates that the minimal conjugated spectroscopic unit (N_{eff}) of **P1** and **P2** must be greater than $N = 50$. Our spectroscopic techniques are not able to distinguish between $N > 50$ and the

average $N = 200\text{--}300$ suggested by the molecular weights. Nevertheless, the spectra and dynamics reported here must be representative of polyenes in the nearly infinite limit.

The electronic properties of correlated π -electrons confined to a quasi-one-dimensional system in a perfect, idealized, infinite polyene are of significant theoretical interest. Recent work by Dincă *et al.* points to a different experimental approach to this limit.⁵⁵ *In situ* synthesis of polyacetylene in a well-ordered urea host crystal produces continuous, extended *all-trans* polyacetylenes with unknown conjugation lengths. Raman bands due to C–C and C=C vibrations largely vanish as the polyene length is increased, consistent with the disappearance both of bond order alternation and the long polyene optical “band gap”. This is a distinctly different limit than described here or in the significant number of previously published papers on polyacetylene and polydiacetylene. Additional experimental and theoretical work will be needed to provide a unified picture of the energies and dynamics of the electronic states of simple polyenes, natural and synthetic carotenoids, and conjugated polymers, including those approaching infinite polyenes.

Conflicts of interest

There are no conflicts to declare.

Acknowledgements

VS and TP thanks the Czech Science Foundation (19-28323X) for financial support. The work at ELI Beamlines was supported by the project Structural Dynamics of Biomolecular Systems (CZ.02.1.01/0.0/0.0/15_003/0000447) from European Regional Development Fund (ELIBIO). TLC acknowledges financial support from the NRF of Korea through a Nano-Material Technology Development Program grant. The authors thank the reviewers for helpful comments relating to the discussion of the conjugation lengths of these samples, and Ondrej Bares for help with preparation of samples for spectroscopy measurements.

Notes and references

- 1 Y. Koyama, F. S. Rondonuwu, R. Fujii and Y. Watanabe, *Biopolymers*, 2004, **74**, 2.
- 2 H. A. Frank, A. Cua, V. Chynwat, A. Young, D. Gosztola and M. R. Wasielewski, *Photosynth. Res.*, 1994, **41**, 389.
- 3 D. Niedzwiedzki, J. F. Kosciielecki, H. Cong, J. O. Sullivan, G. N. Gibson, R. R. Birge and H. A. Frank, *J. Phys. Chem. B*, 2007, **111**, 5984.
- 4 M. M. Mendes-Pinto, E. Sansiaume, H. Hashimoto, A. A. Pascal, A. Gall and B. Robert, *J. Phys. Chem. B*, 2013, **117**, 11015.
- 5 R. L. Christensen, M. M. Enriquez, N. L. Wagner, A. Y. Peacock-Villada, C. Scriban, R. R. Schrock, T. Polívka, H. A. Frank and R. R. Birge, *J. Phys. Chem. A*, 2013, **117**, 1449.
- 6 A. Wand, I. Gdor, J. Zhu, M. Sheves and S. Ruhman, *Annu. Rev. Phys. Chem.*, 2013, **64**, 437.
- 7 T. Mirkovic, E. E. Ostroumov, J. M. Anna, R. Van Grondelle, Govindjee and G. D. Scholes, *Chem. Rev.*, 2017, **117**, 249.
- 8 C. D. P. Duffy and A. V. Ruban, *J. Photochem. Photobiol., B*, 2015, **152**, 215.
- 9 H. Hashimoto, Y. Sugai, C. Urugami, A. T. Gardiner and R. J. Cogdell, *J. Photochem. Photobiol., C*, 2015, **25**, 46.
- 10 T. Polívka and H. A. Frank, *Acc. Chem. Res.*, 2010, **43**, 1125.
- 11 T. Polívka and V. Sundström, *Chem. Rev.*, 2004, **104**, 2021.
- 12 A. Gall, R. Berera, M. T. A. Alexandre, A. A. Pascal, L. Bordes, M. M. Mendes-Pinto, S. Andrianambintsoa, K. V. Stoitchkova, A. Marin, L. Valkunas, P. Horton, J. T. M. Kennis, R. Van Grondelle, A. Ruban and B. Robert, *Biophys. J.*, 2011, **101**, 934.
- 13 T. M. Swager, *Macromolecules*, 2017, **50**, 4867.
- 14 B. S. Hudson, *Materials*, 2018, **11**, 242.
- 15 A. J. Blayney, I. F. Perepichka, F. Wudl and D. F. Perepichka, *Isr. J. Chem.*, 2014, **54**, 674.
- 16 R. Ammenhäuser, A. Helfer and U. Scherf, *Org. Mater.*, 2020, **2**, 159.
- 17 M. Schmidt and P. Tavan, *J. Chem. Phys.*, 2012, **136**, 124309.
- 18 R. L. Christensen, in *The Photochemistry of Carotenoids*, ed. H. A. Frank, A. J. Young, G. Britton and R. J. Cogdell, Kluwer Academic, Dordrecht, The Netherlands, 1999, pp. 137–159.
- 19 K. Schulten and M. Karplus, *Chem. Phys. Lett.*, 1972, **14**, 305.
- 20 B. S. Hudson and B. E. Kohler, *Chem. Phys. Lett.*, 1972, **14**, 299.
- 21 P. Tavan and K. Schulten, *Phys. Rev. B: Condens. Matter Mater. Phys.*, 1987, **36**, 4337–4358.
- 22 R. A. Auerbach, R. L. Christensen, M. F. Granville and B. E. Kohler, *J. Chem. Phys.*, 1981, **74**, 4.
- 23 K. L. D'Amico, C. Manos and R. L. Christensen, *J. Am. Chem. Soc.*, 1980, **102**, 1777.
- 24 R. L. Christensen and B. E. Kohler, *J. Phys. Chem.*, 1976, **80**, 2197.
- 25 B. E. Kohler, C. Spangler and C. Westerfield, *J. Chem. Phys.*, 1988, **89**, 5422.
- 26 R. M. Gavin, C. Weisman, J. K. McVey and S. A. Rice, *J. Chem. Phys.*, 1978, **68**, 522.
- 27 H. Petek, A. J. Bell, Y. S. Choi, K. Yoshihara, B. A. Tounge and R. L. Christensen, *J. Chem. Phys.*, 1993, **98**, 3777.
- 28 H. Petek, A. J. Bell, Y. S. Choi, K. Yoshihara, B. A. Tounge and R. L. Christensen, *J. Chem. Phys.*, 1995, **102**, 4726.
- 29 R. Hemley and B. E. Kohler, *Biophys. J.*, 1977, **20**, 377.
- 30 M. Fuciman, P. Chábera, A. Župčanová, P. Hříbek, J. B. Arellano, F. Vácha, J. Pšenčík and T. Polívka, *Phys. Chem. Chem. Phys.*, 2010, **12**, 3112.
- 31 M. Fuciman, G. Keşan, A. M. LaFountain, H. A. Frank and T. Polívka, *J. Phys. Chem. B*, 2015, **119**, 1457.
- 32 R. Withnall, B. Z. Chowdhry, J. Silver, H. G. M. Edwards and L. F. C. De Oliveira, *Spectrochim. Acta, Part A*, 2003, **59**, 2207.
- 33 M. J. Llansola-Portoles, A. A. Pascal and B. Robert, *J. R. Soc., Interface*, 2017, **14**, 20170504.
- 34 T. Polívka and V. Sundström, *Chem. Phys. Lett.*, 2009, **477**, 1.

- 35 L. Fiedor, Heriyanto, J. Fiedor and M. Pilch, *J. Phys. Chem. Lett.*, 2016, **7**, 1821.
- 36 T. Ritz, A. Damjanović, K. Schulten, J. P. Zhang and Y. Koyama, *Photosynth. Res.*, 2000, **66**, 125.
- 37 T. Wei, V. Balevičius, T. Polívka, A. V. Ruban and C. D. P. Duffy, *Phys. Chem. Chem. Phys.*, 2019, **21**, 23187.
- 38 B. DeCoster, R. L. Christensen, R. Gebhard, J. Lugtenburg, R. Farhoosh and H. A. Frank, *Biochim. Biophys. Acta, Bioenerg.*, 1992, **1102**, 107.
- 39 H. A. Frank, R. Z. B. Desamero, V. Chynwat, R. Gebhard, I. Van Der Hoef, F. J. Jansen, J. Lugtenburg, D. Gosztola and M. R. Wasielewski, *J. Phys. Chem. A*, 1997, **101**, 149.
- 40 H. A. Frank, J. S. Josue, J. A. Bautista, I. Van der Hoef, F. J. Jansen, J. Lugtenburg, G. Wiederrecht and R. L. Christensen, *J. Phys. Chem. B*, 2002, **106**, 2083.
- 41 R. L. Christensen, M. Goyette, L. Gallagher, J. Duncan, B. DeCoster, J. Lugtenburg, F. J. Jansen and I. van der Hoef, *J. Phys. Chem. A*, 1999, **103**, 2399.
- 42 T. Polívka, J. L. Herek, D. Zigmantas, H. E. Åkerlund and V. Sundström, *Proc. Natl. Acad. Sci. U. S. A.*, 1999, **96**, 4914.
- 43 P. O. Andersson and T. Gillbro, *J. Chem. Phys.*, 1995, **103**, 2509.
- 44 V. Balevičius, A. G. Pour, J. Savolainen, C. N. Lincoln, V. Lukeš, E. Riedle, L. Valkunas, D. Abramavicius and J. Hauer, *Phys. Chem. Chem. Phys.*, 2015, **17**, 19491.
- 45 V. Balevičius Jr., D. Abramavicius, T. Polívka, A. Galestian Pour and J. Hauer, *J. Phys. Chem. Lett.*, 2016, **7**, 3347.
- 46 F. Ehlers, M. Scholz, K. Oum and T. Lenzer, *Arch. Biochem. Biophys.*, 2018, **646**, 137.
- 47 T. Lenzer, F. Ehlers, M. Scholz, R. Oswald and K. Oum, *Phys. Chem. Chem. Phys.*, 2010, **12**, 8832.
- 48 R. L. Christensen, A. Faksh, J. A. Meyers, I. D. W. Samuel, P. Wood, R. R. Schrock and K. C. Hultsch, *J. Phys. Chem. A*, 2004, **108**, 8229.
- 49 M. R. Antognazza, L. Lüer, D. Polli, R. L. Christensen, R. R. Schrock, G. Lanzani and G. Cerullo, *Chem. Phys.*, 2010, **373**, 115.
- 50 C. Czekelius, J. Hafer, Z. J. Tonzetich, R. R. Schrock, R. L. Christensen and P. Müller, *J. Am. Chem. Soc.*, 2006, **128**, 16664.
- 51 C. Scriban, B. S. Amagai, E. A. Stemmler, R. L. Christensen and R. R. Schrock, *J. Am. Chem. Soc.*, 2009, **131**, 13441.
- 52 H. Staleva, M. Zeeshan, P. Chábera, V. Partali, H. R. Sliwka and T. Polívka, *J. Phys. Chem. A*, 2015, **119**, 11304.
- 53 D. Kosumi, M. Fujiwara, R. Fujii, R. J. Cogdell, H. Hashimoto and M. Yoshizawa, *J. Chem. Phys.*, 2009, **130**, 214506.
- 54 Z. Chen, J. A. M. Mercer, X. Zhu, J. A. H. Romaniuk, R. Pfattner, L. Cegelski, T. J. Martinez, N. Z. Burns and Y. Xia, *Science*, 2017, **357**, 475.
- 55 S. A. Dincă, D. G. Allis, M. D. Moskowitz, M. B. Sponsler and B. S. Hudson, *Chem. Mater.*, 2020, **32**, 1769.
- 56 E. H. Kang, I. S. Lee and T. L. Choi, *J. Am. Chem. Soc.*, 2011, **133**, 11904.
- 57 E. H. Kang, S. Y. Yu, I. S. Lee, S. E. Park and T. L. Choi, *J. Am. Chem. Soc.*, 2014, **136**, 10508.
- 58 G. I. Peterson, S. Yang and T. L. Choi, *Acc. Chem. Res.*, 2019, **52**, 994.
- 59 H. H. Fox, M. O. Wolf, R. O'Dell, B. L. Lin, R. R. Schrock and M. S. Wrighton, *J. Am. Chem. Soc.*, 1994, **116**, 2827.
- 60 F. J. Schattenmann, R. R. Schrock and W. M. Davis, *J. Am. Chem. Soc.*, 1996, **118**, 3295.
- 61 U. Anders, O. Nuyken, M. R. Buchmeiser and K. Wurst, *Angew. Chem., Int. Ed.*, 2002, **41**, 4044.
- 62 E. H. Kang and T. L. Choi, *ACS Macro Lett.*, 2013, **2**, 780.
- 63 S. S. Rane and P. Choi, *Chem. Mater.*, 2005, **17**, 926.
- 64 I. H. M. Van Stokkum, D. S. Larsen and R. Van Grondelle, *Biochim. Biophys. Acta, Bioenerg.*, 2004, **1657**, 82.
- 65 M. Zeeshan, H. R. Sliwka, V. Partali and A. Martínez, *Org. Lett.*, 2012, **14**, 5496.
- 66 S. Yang, S. Shin, I. Choi, J. Lee and T. L. Choi, *J. Am. Chem. Soc.*, 2017, **139**, 3082.
- 67 C. X. Sheng, K. H. Kim, M. Tong, C. Yang, H. Kang, Y. W. Park and Z. V. Vardeny, *Phys. Rev. Lett.*, 2020, **124**, 17401.
- 68 R. Pandya, Q. Gu, A. Cheminal, R. Y. S. Chen, E. P. Booker, R. Soucek, M. Schott, L. Legrand, F. Mathevet, N. Greenham, T. Barisien, A. Musser, A. W. Chin and A. Rao, *SSRN Electron. J.*, 2020, **1**, 1.
- 69 A. Martínez, M. Zeeshan, A. Zaidi, H. R. Sliwka, K. Razi Naqvi and V. Partali, *Comput. Theor. Chem.*, 2018, **1125**, 133.
- 70 K. R. Naqvi, *J. Phys. Chem. Lett.*, 2016, **7**, 676.
- 71 P. Wood, I. D. W. Samuel, R. Schrock and R. L. Christensen, *J. Chem. Phys.*, 2001, **115**, 10955.
- 72 W. Fuß, Y. Haas and S. Zilberg, *Chem. Phys.*, 2000, **259**, 273.
- 73 H. Nagae, M. Kuki, J. P. Zhang, T. Sashima, Y. Mukai and Y. Koyama, *J. Phys. Chem. A*, 2000, **104**, 4155.
- 74 P. Chábera, M. Fuciman, P. Hřibek and T. Polívka, *Phys. Chem. Chem. Phys.*, 2009, **11**, 8795.
- 75 C. C. Gradinaru, J. T. M. Kennis, E. Papagiannakis, I. H. M. Van Stokkum, R. J. Cogdell, G. R. Fleming, R. A. Niederman and R. Van Grondelle, *Proc. Natl. Acad. Sci. U. S. A.*, 2001, **98**, 2364.